tion for the crystal. The explanation is hidden in the complex compromises made by each of the six R sites, none of which generally has its moment fully aligned, even when the sum of the moments is aligned.

[31]R. Alben, Phys. Rev. Letters 24, 68 (1970); another mention of this kind of point occurs in Ref. 5, but in the case treated there, the mean-field approach is not as well justified as for YbIG.

[32]Near (H_c, T_c) X_F behaves as $q^{1/3}$ for all paths except the coexistence curve $(q=0)$. Along $q=0$, X_F behaves as $p^{1/2}$. It is traditional to denote by δ the exponent which gives the behavior of the forcing variable as a function of the state variable: $t=aX^{\delta}$. The value of δ is 3 for this classical critical point. The variation of X along the coexistence curve is given by the exponent β and here $\beta=\frac{1}{2}$, again the classical value.

[33]For the high temperature here the R-sublattice model of anisotropy is difficult to justify since R is almost demagnetized. Thus, unlike in previous treatments, we here use the F-sublattice model.

[34]However, since there is a change in symmetry the "outer" phase boundary cannot end, it continues as a first-order line. The point F exhibits behavior similar to a second-order line (point D) and not like a liquid-vapor-like point (B).

PHYSICAL REVIEW B VOLUME 2, NUMBER 7 1 OCTOBER 1970

Nuclear Quadrupole Spin-Lattice Relaxation and Critical Dynamics of Ferroelectric Crystals

G. Bonera, F. Borsa, and A. Rigamonti
Istituto di Fisica dell'Università di Pavia,
Gruppo Nazionale di Struttura della Materia del Consiglio Nazionale delle Ricerche, Pavia, Italy 27100

(Received 21 January 1970)

The effect on the nuclear spin-lattice relaxation of the anomalous temperature dependence of generalized unstable lattice modes near the ferroelectric transition is investigated both theoretically and experimentally. Expressions for the relaxation rate near T_c are derived for typical cases of critical dynamics of ferroelectric crystals. For the case of undamped soft-phonon modes it is shown that, on the basis of a Raman two-phonon relaxation mechanism, the relaxation rate should behave near the transition temperature as $(T-T_0)^{-n}$, where n depends on the shape of the dispersion curve of the soft branch. On the other hand, for the case of damped-oscillatory modes or diffusive modes, the relaxation rate, derived by using the classical approach for the direct relaxation process, should behave as $(T-T_0)^{-1/2}$ or as $\ln(T-T_0)$ if the anisotropic character of the dipolar interaction is taken into account. An experimental investigation of the nuclear spin-lattice relaxation rate in $NaNO_2$ single crystal is presented. The resonance spectrum and the recovery law under different conditions are discussed. The results of the relaxation rate as a function of temperature, angular orientation, and resonance frequency indicate the existence of a damped generalized soft mode or critical diffusive mode. The available data on the shape of the relaxation-rate peak tends to favor the logarithmic singularity, in agreement with the prediction of an anisotropic interaction. From the analysis of the data, it is inferred that the soft mode can be identified as the flipping motion along the ferroelectric c axis of the electric dipoles associated with the NO_2^- group, which seem to be mainly correlated along the a axis. The relaxation measurements support the recent suggestion for a new low-temperature phase transition.

I. INTRODUCTION

Nuclear magnetic resonance (NMR) techniques have been widely employed in order to gain information on the phase transition and on the properties of ferroelectric crystals.[1] Information on structural or symmetry changes occurring at the phase transition can be obtained from the splitting and/or shift of the NMR spectrum associated with the static quadrupole interaction with the lattice. Furthermore from the temperature dependence of the quadrupole interaction one can deduce the temperature dependence of the spontaneous polarization. The temperature dependence of the jumping frequency of atoms between sites with different electric-field gradients (efg) can be evidenced by the collapsing of the corresponding resonance lines. Finally, measurements of spin-lattice relaxation time governed by magnetic dipolar interactions and quadrupole interactions have been performed, mainly in hydrogen-bonded ferroelectrics, in order to study the proton or deuteron motion both in the paraelectric and ferroelectric phases.

In ordinary diamagnetic nonconducting ferroelectrics the main source of relaxation for nuclei with $I>\frac{1}{2}$ is the coupling between the nuclear-spin system and the crystal lattice through the interaction

of the nuclear-quadrupole moment with the efg in the crystal; the coupling is made time dependent by the different characteristic motions in the crystal. Therefore, measurements of quadrupole relaxation provide information about the dynamical properties of the crystal, whose importance in the understanding of the microscopic mechanism of the ferroelectric transition has been emphasized in recent years. In fact, Anderson[2] and Cochran[3] explained the transition in displacive ferroelectrics in terms of a lattice instability arising from the anomalous frequency lowering of a long-wavelength transverse-optical mode near the Curie point. Also in order-disorder hydrogen-bonded ferroelectrics the transition to the polar state has been described by Brout, Müller, and Thomas,[4] in the framework of a quasi-spin-wave formalism,[5] on the basis of low-lying collective excitations whose frequency exhibits a critical behavior. Finally in mixed-type ferroelectric crystals, where a coupling between the tunneling or flipping motion of the ions and a phonon mode is taken into account, Kobayashi[6] has shown that the ferroelectric transition is driven by the anomalous temperature behavior of the frequency of a coupled quasi-spin-wave phonon mode.

Recently a study of quadrupole relaxation in a ferroelectric crystal was performed by one of us.[7] Measurements in powdered sodium nitrite showed a peak in the relaxation rate near the transition temperature. The results were interpreted semiquantitatively in terms of quadrupole relaxation induced by lattice vibrations through a Raman two-phonon mechanism and it was speculated that the ferroelectric contribution, i.e., the anomalous increase in the relaxation rate near the transition, is associated with the frequency lowering of a soft ferroelectric mode. Subsequently Blinc and Zumer[8] observed an analogous ferroelectric contribution in the nuclear magnetic spin-phonon relaxation of P^{31} in KH_2PO_4. These authors interpreted the ferroelectric contribution by relating, in the classical spectral-density approach, the magnetic relaxation to the long-wavelength electrical-polarization fluctuations. The spectral density is obtained by the fluctuation-dissipation theorem on the assumption that the generalized dielectric susceptibility is the one pertaining to a system of single-damped harmonic oscillators. However Blinc and Zumer overestimated the ferroelectric contribution by considering only the long-wavelength ($q = 0$) polarization fluctuations. The above theoretical approach has been recently employed by us[9] in order to describe the quadrupole ferroelectric contribution from strongly damped phonon modes and from the statistical flipping motion of interacting electric dipoles by taking into account, in an approximate way, also the contribution coming from modes with $q \neq 0$. An anomaly of the nuclear spin-lattice relaxation rate near the critical temperature was also observed by us[10] in Rochelle Salt and sodium-tungsten bronzes (Na_xWO_3).

In this paper we present an elaboration of the theory of the quadrupole relaxation in ferroelectric crystals and an experimental investigation in single-crystal sodium nitrite. A theoretical treatment, similar to the one which will be given in Sec. II B, will be presented also by Blinc *et al.*[11] in connection with measurements of magnetic relaxation in dicalcium strontium propionate.

In Sec. II the outlines of the theory of nuclear relaxation by quadrupole interaction in a ferroelectric crystal are given; in Sec. II A an expression of the relaxation rates for a Raman second-order two-phonon mechanism is derived for two typical dispersion curves for the ferroelectric branch; in Sec. II B the relaxation transition probabilities are calculated in the framework of the classical lattice approach where the spectral density is obtained by relating the efg fluctuations to the polarization fluctuations and then, by making use of the fluctuation-dissipation theorem, to the generalized dielectric susceptibility. All q components of the polarization are taken into account by assuming an approximate expression for the q dependence of the generalized susceptibility both for the cases of isotropic and anisotropic interaction. The experimental details and the methods of analysis of the raw experimental data are presented in Sec. III. This section has been developed to some length because the measurements of quadrupole relaxation in noncubic crystals are not straightforward. The experimental results and their discussion are presented in Sec. IV, while in Sec. V the conclusions are summarized.

II. THEORY

In general two approaches can be used to describe the quadrupole spin-lattice relaxation; one is based on a quantum description of the lattice while the other is based on a classical lattice. The first approach, employing Van Kranendonk's[12] Raman second-order two-phonon process, is used in Sec. II A. It appears suitable to derive the ferroelectric contribution to the relaxation rate in a crystal where the ferroelectric transition is related to the existence of soft underdamped phonon-lattice modes. However, in order-disorder or mixed-type ferroelectric crystals, where in general a more complex dynamics triggers the phase transition, a quantization of the lattice cannot be easily given and the classical lattice approach should be used. The treatment for this second

case is developed in Sec. IIB by expressing the nuclear relaxation in terms of the spectral density of the spin-lattice interaction[13] where the spectral density is then evaluated in terms of the appropriate microscopic critical dynamics of the system.

It may be noted that the classical lattice approach describes a direct relaxation process while the Raman two-phonon mechanism is an indirect relaxation process. The relaxation due to the indirect process is predominant for underdamped phonons, while for strongly damped phonons or for a purely relaxation-type motion the direct process should give the more relevant contribution.[14]

A. Indirect Raman Two-Phonon Mechanism

In the Raman relaxation process the spin transition between Zeeman levels m and $m+\mu$ is accompanied by the creation of a phonon and the annihilation of another whose frequency differs by $\mu\omega_L$ (ω_L = Larmor frequency). The transition probability is obtained by integrating over the phonon-frequency spectrum,

$$W_{m,m+\mu}=(2\pi/\hbar^2)\sum\int\int(|\langle m,n_i+1,\ n_j-1\,|\,\mathcal{H}_Q^{(2)}\,|n_i,n_j,m+\mu\rangle|^2)\rho(\omega_i)\rho(\omega_j)\delta(\omega_i-\omega_j-\mu\omega_L)d\omega_i\,d\omega_j\,, \tag{1}$$

where $\mathcal{H}_Q^{(2)}$ is the effective quadrupole Hamiltonian, which couples the nucleus with the lattice, n_i and n_j are the phonon quantum numbers, and $\sum$ stands for a summation over the phonon branches; the contribution to relaxation has been considered independently for each of the acoustic and optical branches; the curled brackets stand for an average over all directions of phonon propagation. The contribution to the relaxation rate coming from each branch depends on the phonon-frequency spectrum and several calculations have been performed using approximate forms of the spectrum.[15] It has been shown that in the high-temperature approximation the results are rather insensitive to the details of the phonon spectrum. However, as will be shown, the drastic changes of the ferroelectric branch, near the transition temperature, can affect the relaxation rate in a ferroelectric crystal.

In Eq. (1) the temperature enters only through the equilibrium-phonon occupation numbers and thus, in the high-temperature approximation, i.e., $kT\gg\hbar\omega_{\max}$, the transition probability is of the form $W\propto T^2$ for any branch and any type of phonon spectrum assumed, as long as the latter is almost temperature independent. Let us consider the transverse-optical branch (TO) which is characterized by an anomalous temperature behavior and discuss its contribution in detail. Equation (1) can be rewritten

$$W_{m,m+\mu}=KT^2+(2\pi/\hbar^2)\,|\,Q_{\mu m}\,|^2 \times\int_{\mathrm{TO}}(|\langle n_i+1,\ n_j-1|\,V_{-\mu}^{(2)}\,|n_i,\ n_j\rangle|^2)\rho_{\mathrm{TO}}^2(\omega)\,d\omega, \tag{2}$$

where all contributions, with the exception of the one coming from the ferroelectric branch, are included in the term KT^2. In Eq. (2) we have assumed $\omega_i,\ \omega_j\gg\mu\omega_L$. The quadrupole Hamiltonian was written as

$$\mathcal{H}_Q=\sum_\mu Q_\mu V_{-\mu}\,,\qquad \mu=0,\pm1,\pm2, \tag{3}$$

where

$$\begin{aligned} Q_0&=A(3I_z^2-I^2)\,, & V_0&=V_{zz}\,,\\ Q_{\pm1}&=A(I_\pm I_z+I_zI_\pm)\,, & V_{\pm1}&=V_{xz}\pm iV_{yz}\,,\\ Q_{\pm2}&=AI_\pm^2\,, & V_{\pm2}&=\tfrac{1}{2}(V_{xx}-V_{yy})\pm iV_{xy} \end{aligned} \tag{4}$$

with $A=eQ/4I(2I-1)$, V_{ij} the efg components and $Q_{\mu m}=\langle m\,|\,Q_\mu\,|\,m+\mu\rangle$.

The term in the Hamiltonian (3) that corresponds to the Raman two-phonon process is the term quadratic in the lattice displacements in the expansion of V_μ in terms of lattice displacements $\vec{u}$ from the equilibrium positions; i.e.,

$$\begin{aligned} V_\mu^{(2)}&=\tfrac{1}{2}\sum_{\alpha\beta}\sum_{tt'}\sum_{ij}\left(\frac{\partial^2V_\mu}{\partial r_\alpha^t\,\partial r_\beta^{t'}}\right)_0\frac{\partial u_\alpha^t}{\partial Q_i}\frac{\partial u_\alpha^{t'}}{\partial Q_j}Q_iQ_j\\ &\equiv\tfrac{1}{2}\sum_{ij}\frac{\partial^2V_\mu}{\partial Q_i\,\partial Q_j}Q_iQ_j\,, \end{aligned} \tag{5}$$

where r_α^t is the α component of the position vector of the tth ion, $\vec{u}^{\,t}$ is the displacement from the equilibrium position, and Q_i is the normal coordinate relative to the ith normal mode of the ferroelectric transverse-optical branch, which is not to be confused with the quadrupole moment operator defined in Eq. (4).

From Eq. (5), by using the expressions for the matrix elements of Q,

$$\langle n+1\,|\,Q\,|\,n\rangle=\langle n\,|\,Q\,|\,n+1\rangle=(\hbar/M\omega)^{1/2}(n+1)^{1/2},$$

where M is the mass of the crystal and

$$\bar{n}=(e^{\hbar\omega/kT}-1)^{-1}\simeq kT/\hbar\omega\,,$$

one obtains

$$W_{m,m+\mu}=KT^2+\frac{2\pi}{\hbar^2}\,|\,Q_{\mu m}|^2BT^2\int_{\mathrm{TO}}\frac{\rho_{\mathrm{TO}}^2(\omega)}{\omega^4}\,d\omega\,, \tag{6}$$

where

$$B = (k^2/4M^2)\left\langle\left(\frac{\partial^2 V_\mu}{\partial Q^2}\right)^2\right\rangle_Q ,$$

and we have replaced the derivative of V_μ with respect to the normal coordinate with an average value independent of Q. Therefore the constant B depends on the structure of the crystal and on the different sources for the fluctuating efg which are associated with the optical lattice vibrations (point charges, induced dipoles, covalency, and overlap effects).[15]

In order to perform the integration in Eq. (6) one should make assumptions about the phonon dispersion curve $\omega_{TO}(\vec{q})$ and consequently $\rho_{TO}(\omega)$. If one uses for $\omega_{TO}(\vec{q})$ the function employed by Kochelaev[16] for the optical branches

$$\omega_{TO}(q) = \Delta\omega(q/q_M) + \omega_0 \quad \text{with} \quad \Delta\omega = \omega_M - \omega_0, \tag{7}$$

where ω_M is the frequency corresponding to the maximum value q_M of the wave vector, one obtains for the ferroelectric contribution to the relaxation rate,

$$W^{TO}_{m,m+\mu} = (10\pi^3\hbar^2)^{-1}|Q_{\mu m}|^2 B T^2 (q_M^6/\Delta\omega\omega_0^4). \tag{8}$$

However, in evaluating Eq. (8) we have assumed $\omega^{-4} \simeq \omega_0^{-4}$ for every q, which is a good approximation if $\Delta\omega \ll \omega_0$. This model for optical modes is practically equivalent to an Einstein model where $\Delta\omega$ is the spread in the phonon-frequency spectrum which one has to assume in order to allow a Raman process.

By imposing in Eq. (8) Cochran's condition for the occurrence of the ferroelectric transition, i.e., $\omega_0^2 = \beta(T - T_0)$ for $T > T_0$ and assuming $\Delta\omega$ temperature independent, we obtain for the relaxation rate due to the ferroelectric branch the relation

$$W^{TO'}_{m,m+\mu} = \frac{18\pi}{5\hbar^2}|Q_{\mu m}|^2 B \frac{N^2\xi^2}{\Delta\omega}\frac{T^2}{\beta^2(T - T_0)^2} . \tag{9}$$

It should be stressed that this model overestimates the effect of the lowering of the frequency of the ferroelectric branch. In fact it corresponds to imposing Cochran's condition on all the modes of the branch. This overestimation can be in part compensated by limiting q_M to a value q^* which includes only a fraction $\xi = q^{*3}/6\pi^2 N$ of the total number N of modes in the ferroelectric branch, as we have done in writing Eq. (9).

Another possible expression for the dispersion curve is

$$\omega_{TO}(q) = (\Delta\omega/q^{*2})q^2 + \omega_0, \quad 0 \le q \le q^* .$$

In this case, by performing the integration in Eq. (6), one obtains

$$W^{TO'}_{m,m+\mu} = \frac{3\pi}{4\hbar^2}|Q_{\mu m}|^2 B T^2 \frac{\xi^2 N^2}{(\Delta\omega)^3}\left(\frac{1}{\omega_0^2} - \frac{2\Delta\omega}{\omega^{*3}} - \frac{1}{\omega^{*2}}\right). \tag{10}$$

By putting Cochran's condition in Eq. (10) the relaxation rate contains a singular term of the form

$$W^{TO'}_{m,m+\mu} \propto [T^2/(T - T_0)] \quad \text{for } T > T_0 . \tag{11}$$

By assuming a still different dispersion curve of the form

$$\omega^2_{TO}(q) = [(\omega^{*2} - \omega_0^2)/q^{*2}]\, q^2 + \omega_0^2 ,$$

we obtain that for T near T_0 the relaxation rate approaches the function $C_1 - C_2(T - T_0)^{1/2}$, which remains finite at T_0 although its derivative does not.

One can conclude that the Raman two-phonon relaxation contribution associated with the ferroelectric branch displays a peak in the relaxation rate near T_0 whenever the frequency at $q = 0$ of the phonon spectrum is assumed to go to zero on approaching the ferroelectric transition. The shape of the peak however, is a rather sensitive function of the phonon spectrum assumed.[17]

B. Direct Relaxation Mechanism

Let us consider the case where the nuclear relaxation is due to the efg fluctuations associated with the cooperative motion of permanent electrical dipoles or of tunneling ions.

The quadrupole spin-lattice relaxation transition probability is written[13]

$$W_{m,m+\mu} = (1/\hbar^2)|Q_{\mu m}|^2 J_\mu(\mu\omega_L), \tag{12}$$

where the spectral density $J_\mu(\omega)$ is given by

$$J_\mu(\omega) = \int_{-\infty}^{+\infty} e^{-i\omega t}\langle V_\mu(0)V_\mu^*(t)\rangle\, dt . \tag{13}$$

If one considers that the permanent electrical dipoles can flip between two opposite positions along a given direction or that the ions tunnel between two equilibrium sites, then the time-dependent part of the efg function V_μ at the nuclear position can be written in the form

$$V_\mu(t) = \tfrac{1}{2}\textstyle\sum_i A_\mu^{(i)}\sigma_i(t), \tag{14}$$

where $\sigma(t)$ assumes the values ± 1 and $A_\mu^{(i)}$ is the difference between the two values of the efg function V_μ due to the ith dipole moment (or tunneling ion) in the two positions.

By expanding in Fourier components we obtain in the random-phase approximation

$$J_\mu(\omega) = (4N)^{-1}\textstyle\sum_{\vec{q}} A_\mu(\vec{q})A_\mu^*(\vec{q}) \times \displaystyle\int_{-\infty}^{+\infty} e^{-i\omega t}\,\langle\sigma(\vec{q},0)\sigma(-\vec{q},t)\rangle\, dt , \tag{15}$$

where

$$\sigma(\vec{q},t) = (N)^{-1/2}\textstyle\sum_i \sigma_i(t)e^{i\vec{q}\cdot\vec{r}_i} , \qquad A_\mu(\vec{q}) = \textstyle\sum_i A_\mu^{(i)} e^{i\vec{q}\cdot\vec{r}_i} \tag{16}$$

The spectral density of the time-dependent func-

tion $\sigma(\vec{q}, t)$ can be related by the fluctuation-dissipation theorem to the imaginary part of the reduced generalized dielectric susceptibility $\chi(\vec{q}, \omega)$:

$$\int_{-\infty}^{+\infty} e^{-i\omega t} \langle \sigma(\vec{q}, 0)\sigma(-\vec{q}, t)\rangle dt = -(2kT/N\omega)\chi''(\vec{q}, \omega) . \quad (17)$$

From Eqs. (12), (13), (15), and (17) one obtains for the spin-lattice relaxation rate the expression

$$W_{m,m+\mu} = (\hbar^2)^{-1} |Q_{\mu m}|^2 (kT/2\mu\omega_L) N^{-2} \times \sum_{\vec{q}} A_\mu(\vec{q}) A_\mu^*(\vec{q}) \chi''(\vec{q}, \mu\omega_L) . \quad (18)$$

Since on approaching the transition temperature only the low q values of the susceptibility are strongly enhanced, and the efg goes as r^{-4}, so that mainly the nearest neighbors contribute to $A_\mu(\vec{q})$, in performing the q summation in Eq. (18) we will set $A_\mu(\vec{q}) = A_\mu(0)$.[18] Then the evaluation of the relaxation rate is reduced to the evaluation of

$$I = \sum_{\vec{q}} \chi''(\vec{q}, \omega) , \quad (19)$$

which we will do for a diffusive-mode model and a generalized damped-oscillator soft-mode model. The evaluation will be done in the assumption of an isotropic interaction; subsequently, the anisotropic effect will be discussed.

1. *Diffusive-Mode Model*

If one assumes that the electric dipoles can be considered an interacting Ising spin system (where the Ising variable corresponds to the two equilibrium positions), the dynamical susceptibility can be written in the form[19]

$$\chi(\vec{q}, \omega) = \chi(\vec{q}, 0)/[1 + i\omega\tau(\vec{q})] , \quad (20)$$

with

$$\chi(\vec{q}, 0) = (N/kT)[\tau(\vec{q})/\tau_0] ,$$

where the q-dependent dielectric relaxation time $\tau(\vec{q})$ is related to the Fourier transform of the dipole-dipole interaction J_{ij} by the relation

$$\tau(\vec{q}) = \tau_0/[1 - \beta J(\vec{q})] \quad [\beta \equiv (1/kT)] , \quad (21)$$

and τ_0 is the relaxation time for the noninteracting dipole system.

Expression (19) becomes

$$I(\mu\omega_L) = \frac{\beta N}{\tau_0} \sum_{\vec{q}} \frac{\mu\omega_L \tau^2(\vec{q})}{1 + \mu^2\omega_L^2 \tau^2(\vec{q})} . \quad (22)$$

For isotropic interaction by approximating $J(q) = J(0)(1 - \alpha q^2)$ and by integrating over the Debye zone, we obtain in the case of $[\mu\omega_L\tau(q)]^2 \ll 1$,

$$I(\mu\omega_L) = \frac{VN\tau_0\beta\mu\omega_L}{4\pi^2} \left(\frac{T}{T_0}\right)^2 \frac{1}{\alpha^{3/2}} \times \left[\left(\frac{T_0}{T - T_0}\right)^{1/2} \tan^{-1}(\alpha)^{1/2} q_D \left(\frac{T_0}{T - T_0}\right)^{1/2} - (\alpha)^{1/2} q_D \frac{T_0}{T - T_0(1 - \alpha q_D^2)}\right] , \quad (23)$$

where $T_0 = J(0)/k$ is the Curie temperature and $q_D = (6\pi^2/V)^{1/3}$. Near the transition temperature the quadrupole spin-lattice relaxation rate [see Eq. (18)] assumes the approximate expression

$$W_{m,m+\mu} = A\left[\left(\frac{T_0}{T - T_0}\right)^{1/2} - \frac{4}{\pi(\alpha)^{1/2} q_D}\right] \quad (24)$$

$$\text{for } \left[(\alpha)^{1/2} q_D \left(\frac{T_0}{T - T_0}\right)^{1/2}\right]^3 \gg 1 ,$$

$$A = \frac{1}{16\pi\hbar^2} |Q_{\mu m}|^2 (\textstyle\sum_i A_\mu^{(i)})^2 \tau_0 \left(\frac{T}{T_0}\right)^2 \frac{V}{N\alpha^{3/2}} .$$

2. *Generalized Damped-Oscillator Soft-Mode Model*

The susceptibility can be written in the form[20]

$$\chi(\vec{q}, \omega) = \chi(\vec{q}, 0)\omega^2(\vec{q})/[(\omega^2(\vec{q}) - \omega^2) + i2\Gamma\omega] , \quad (25)$$

$$\chi(\vec{q}, 0) = \lambda/\omega^2(\vec{q}) ,$$

where $\omega(\vec{q})$ is the frequency and Γ is the damping factor of the soft modes. The q dependence of the frequency of the soft modes can be approximated as

$$\omega^2(q) = a(T - T_0) + \gamma q^2 . \quad (26)$$

Since we are interested in the value of the susceptibility at the Larmor frequency we point out that for $\mu\omega_L \ll \omega(q)$ and an appreciably large damping the susceptibility turns out to be of the Debye type [see Eq. (20)] with $\tau(q) = 2\Gamma/\omega^2(q)$. Therefore in the case in which the frequency of the soft mode $\omega(q)$ remains greater than $\mu\omega_L$ even close to T_0, one obtains for the ferroelectric contribution to the relaxation rate

$$W_{m,m+\mu} = B\left[\left(\frac{T_0}{T - T_0}\right)^{1/2} - \frac{4(aT_0)^{1/2}}{\pi(\gamma)^{1/2} q_D}\right] , \quad (27)$$

$$B = \frac{1}{16\pi\hbar^2} |Q_{\mu m}|^2 (\textstyle\sum_i A_\mu^{(i)})^2 \frac{V\lambda kT 2\Gamma}{N^2\gamma^{3/2}} (aT_0)^{-1/2} .$$

3. *Anisotropic Interaction*

An evaluation of the generalized susceptibility $\chi(\vec{q}, \omega)$ for the case of the anisotropic dipolar interaction was performed by Pytte and Thomas.[21] In the light of their results we assume in Eq. (21),

$$J(\vec{q}) = J(0)[1 - \alpha q^2 - \delta \cos^2\theta] , \quad (28a)$$

and instead of Eq. (26),

$$\omega^2(\vec{q}) = a(T - T_0) + \gamma q^2 + \epsilon \cos^2\theta \quad , \tag{28b}$$

where θ is the angle between the $\vec{q}$ vector and the ferroelectric axis (assumed to be a symmetry axis of the crystal). By performing the summation (19), for the case of the Suzuki-Kubo dynamics, we obtain for the singular part of the ferroelectric contribution near the transition temperature,

$$W_{m,m+\mu} = A\delta^{-1/2}\{\ln[T_0/(T - T_0)]^{1/2} + \ln\{[T/T_0 - (1-\delta)]^{1/2} + (\delta)^{1/2}\}\} - A[4/\pi(\alpha)^{1/2}q_D], \tag{29a}$$

where the constant A is the same as in Eq. (24).

For the case of damped harmonic oscillators with $\omega^2(\vec{q})$ given by Eq. (28b) one obtains

$$W_{m,m+\mu} = B\left(\frac{aT_0}{\epsilon}\right)^{1/2}\left\{\ln\left(\frac{T_0}{T - T_0}\right)^{1/2} + \ln\left\{\left[\frac{T}{T_0} - \left(1 - \frac{\epsilon}{aT_0}\right)\right]^{1/2} + \left(\frac{\epsilon}{aT_0}\right)^{1/2}\right\}\right\} - B\left(\frac{4(aT_0)^{1/2}}{\pi(\gamma)^{1/2}q_D}\right) \quad , \tag{29b}$$

where B is the same as in Eq. (27).

As can be seen from Eqs. (29a) and (29b) for $\delta \sim 1$ or $\epsilon/aT_0 \sim 1$, respectively, the singularity in the relaxation rates is logarithmic, while for $\delta \ll 1$ or $\epsilon/aT_0 \ll 1$ one recovers the square-root singularity valid for isotropic interaction. A logarithmic singularity was obtained for the specific heat by Pytte and Thomas[21] who used a more general expression for $\omega^2(\vec{q})$ in the case of anisotropic dipolar forces.

The condition $\mu\omega_L \ll \omega(q)$ or $1/\tau(q)$, used in performing the above calculations, breaks down if the frequency of the soft modes reaches a value of the order of the Larmor frequency before the transition occurs. In this case an appreciable dependence of the relaxation rates on the measuring frequency should be observed. The nuclear relaxation rate in the case of a diffusive mode decreases at given temperature by increasing the measuring frequency, as it can be inferred from Eqs. (18) and (22). On the contrary, for generalized soft modes with no overdamping, the frequency dependence is opposite [Eq. (25)].

III. EXPERIMENTAL DETAILS AND ANALYSIS OF RESULTS

A. Experimental

The Na^{23} nuclear spin-lattice relaxation in sodium nitrite has been investigated, by NMR pulse techniques, in powdered and single crystal.[22] The measurements were performed with a Brüker B-KR 306 coherent pulse spectrometer operating at 24 and 8 MHz; the maximum intensity available for the rf field H_1 was 30–60 Oe, respectively. The transient nuclear signal was detected by direct observation on the oscilloscope or recorded by a box-car integrator. In order to avoid the nonlinearity effects due to the diode detection, a constant reference signal of proper phase and amplitude was added to the nuclear signal or a calibrated correction curve was used.

The temperature was varied by a standard nitrogen-gas flow system and it was measured with the thermocouple junction in thermal contact with the upper part of the sample; the temperature was stable within 1 °C. The spurious "piezoelectric" signal superimposed on the free precession decay was suppressed by loading the sample surface with a liquid.

The relaxation-rate measurements were performed by the usual 90°, t, 90° pulse method. The first pulse produces the equalization of the population of the irradiated Zeeman levels; the amplitude $S(t)$ of the nuclear free precession signal following the second 90° pulse yields the relative population difference at the time t during the recovery process. In order to extract from the experiment the $\Delta m = 1$, 2 relaxation transition probabilities W_1 and W_2 one has to know the recovery law, which depends on the Zeeman levels that are irradiated.

For a nucleus with $I = \frac{3}{2}$ in presence of static quadrupole interaction, three resonance lines corresponding, respectively, to the $+\frac{1}{2} \leftrightarrow -\frac{1}{2}$ transitions (central line) and $\pm\frac{3}{2} \leftrightarrow \pm\frac{1}{2}$ transitions (satellite lines) are generally observed. The resonance frequency of the satellite lines is shifted in first order according to[23]

$$\nu_s - \nu_L = \pm\tfrac{1}{2}\nu_Q(3\cos^2\theta - 1) \quad , \tag{30}$$

while for the central line only second-order terms are effective and the shift is

$$\nu_c - \nu_L = \tfrac{3}{16}(\nu_Q^2/\nu_L)(1 - \cos^2\theta)(1 - 9\cos^2\theta) \quad , \tag{31}$$

where $\nu_Q = e^2qQ/2h$ and $eq \equiv V_{zz}$ is the largest component of the diagonalized efg tensor; θ is the polar angle of the steady magnetic field in the principal axes frame of reference Σ^P of the efg tensor. Therefore several different cases for the recovery law can be considered. For the case in which only the central line is irradiated, by solving the master equations with the appropriate initial conditions, one has for the recovery law

$$[S(\infty) - S(t)]/S(\infty) = \tfrac{1}{2}(e^{-2W_1 t} + e^{-2W_2 t}) \quad . \tag{32a}$$

For irradiation of one satellite line one has

$$[S(\infty)-S(t)]/S(\infty)=\tfrac{1}{2}[e^{-2W_1t}+e^{-2(W_1+W_2)t}]\ , \quad (32b)$$

while for simultaneous irradiation of all lines

$$[S(\infty)-S(t)]/S(\infty)=e^{-2/5(W_1+4W_2)t}\ . \quad (32c)$$

B. $NaNO_2$ Measurements

Sodium nitrite is a ferroelectric crystal with body-centered orthorhombic structure (space group $C_{2v}^{20}Imm2$). The transition to the nonpolar centro-symmetric phase (space group $D_{2h}^{25}Immm$) occurs[24] at ~164 °C; the transition is accompanied by an order-disorder rearrangement relative to the orientation of the NO_2^- radicals and a displacement of the Na^+ ions along the ferroelectric c axis.[25]

The static quadrupole effects have been previously studied by Weiss[26] as a function of temperature; the principal axes of the efg tensor are oriented, in both phases, as the crystal axes ($\vec{z}//\vec{c}$; $a<b<c$); the quadrupole-coupling constant decreases for increasing temperature with a small abrupt change at the transition.[27] Two representative values for the strength of the quadrupole interaction are $\nu_Q=550$ KHz at 18 °C and $\nu_Q=430$ KHz at 166 °C; the asymmetry parameter η is always small ($|\eta|\leq 0.1$) and it changes sign on crossing the transition temperature.

The quadrupole strength and the dipolar line width $\delta\nu_d$ in $NaNO_2$ at any temperature are such that the conditions

$$\nu_Q^2/2\nu_L \ll \gamma H_1\ , \quad (33a)$$

$$\delta\nu_d \ll \gamma H_1 \ll \nu_Q \quad (33b)$$

can be achieved. Therefore, in a single crystal it is possible to irradiate separately central or satellite lines [condition (33b)] or irradiate all lines together [condition (33a)] by choosing a proper orientation of the crystal. In the second case it is convenient to use a comb of 90° pulses instead of the single first pulse in order to be sure to have achieved initial conditions corresponding to a complete saturation of all levels. Moreover, since both the above conditions are sufficiently satisfied at 24 MHz for $H_1\sim 30$ Oe, in a powdered crystal one 90° pulse at the Larmor frequency practically involves irradiation of the central line alone.[7]

In Fig. 1 the Na^{23} free precession (fp) signals for $NaNO_2$ powdered and single crystal at room temperature are shown. For the powdered sample [Fig. 1(a)] and the single crystal, in the case of irradiation of the central line only [Fig. 1(b)], the maximum amplitude of the fp signal was found to correspond to a pulse duration of about $\frac{1}{2}\tau_{\pi/2}$, where $\tau_{\pi/2}$ is the duration of the maximizing pulse for the usual case of all lines superimposed. For irradiation of one of the satellite lines [Fig. 1(c)] the corresponding maximizing pulse is $1/\sqrt{3}\tau_{1/2\pi}$. This result agrees with the pulse durations which can be evaluated by using the fictitious spin-$\frac{1}{2}$ approach.[13]

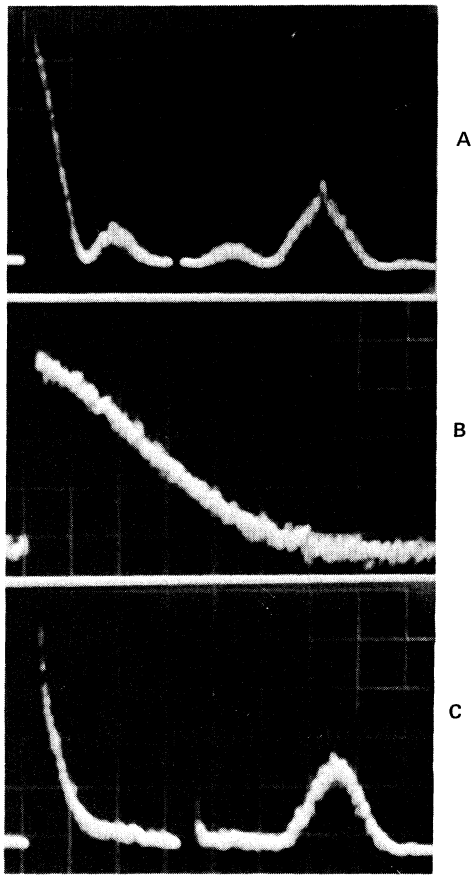

FIG. 1. Na^{23} pulsed NMR signals in $NaNO_2$ at 24 MHz and at room temperature. (a) Free precession (fp) and echo signal in powdered sample with diode detection; (b) fp in single crystal for central-line irradiation; (c) fp and echo in single crystal for a satellite-line irradiation. (The time base is 100 μs/div.)

The fast decay of the fp signal in powdered sample is associated with the different second-order quadrupole shifts [see Eq. (31)] for the various randomly oriented crystallites. Since this broadening is inhomogeneous the decay signal can be refocused into an echo by applying a second pulse [see Fig. 1(a)]. Furthermore the fp decay and echo signal show beats as one expects since the free precession is the Fourier transform of the resonance frequency distribution function. If one neglects the dipolar interaction one can calculate numerically the fp shape. For the time τ^* at which the first minimum appears, in the diode-detected signal, one finds for $\eta<0.2$:

$\tau^* \cong 1.5(\nu_L/\nu_Q^2)$.

The experimental value $\tau^* \simeq 1.2\times10^{-4}$ sec (at 24 MHz) agrees with the quadrupole-coupling constant previously measured[26] if one takes into account the dipolar interaction.

The fp of the satellite line in a single crystal [see Fig. 1(c)] decays more rapidly than the fp of the central line [Fig. 1(b)] and can be refocused into an echo. The dephasing time of the satellite line is angular dependent and it decreases strongly on approaching the transition temperature. This effect can be attributed to a first-order broadening due to lattice defects and to temperature gradients over the sample.[26]

The measurements of relaxation rate as a function of temperature were performed in the single crystal by studying the return to equilibrium conditions in the case of irradiation of all lines superimposed. According to Eq. (32c) the recovery law is exponential with time constant $1/T_1 = \frac{2}{5}(W_1 + 4W_2)$ as is shown in Fig. 2(a).

The study of the angular dependence of the relaxation transition probabilities was limited to the case of a rotation of the crystal around the c axis, with $\vec{c} \perp \vec{H}_0$, so that the central and satellite lines could be irradiated separately at all angles. In principle it is possible to obtain for all angles the relaxation transition probabilities W_1 and W_2 separately. In fact from the tangent at the origin of the nonexponential recovery plot one obtains the quantity $(W_1 + W_2)^{-1}$ for the central line [see Eq. (32a)] and the quantity $(2W_1 + W_2)^{-1}$ for the satellite line [see Eq. (32b)]. However since the quadrupole broadening of the satellite line is too strong for certain orientations, particularly near the transition temperature, we chose to study only the angular dependence of the quantity $W_1 + W_2$ by studying the recovery of the central line [see Fig. 2(b)].

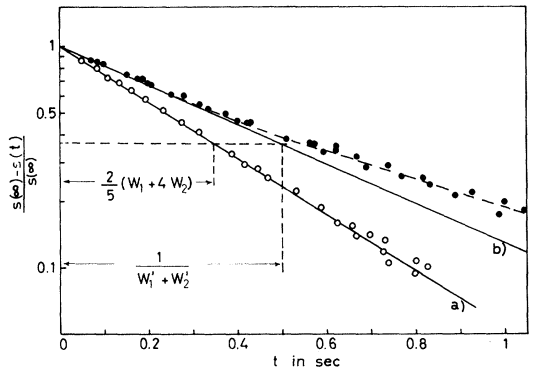

FIG. 2. Semilogarithmic recovery plot as a function of time for Na^{23} in $NaNO_2$ single crystal at room temperature and at 24 MHz. (a) Irradiation of all lines superimposed; (b) irradiation of central line, for an orientation of the crystal with $\vec{c} \perp \vec{H}_0$ and $\vec{b} \hat{} \vec{H}_0 = 90°$.

IV. RESULTS AND DISCUSSION

The temperature dependence of the relaxation rate for a single crystal of $NaNO_2$ is shown in Fig. 3. While approaching the transition temperature from the paraelectric region the relaxation rate (at 24 MHz) rises rapidly by a factor of 4–5, below the transition temperature $1/T_1$ drops rather abruptly, and then keeps decreasing according to a T^2 law. An unexpected anomalous decrease of the relaxation rate by an order of magnitude occurs in the temperature range 220–170 °K. Preliminary measurements of Na^{23} quadrupole-coupling constant were performed in this temperature range but no discontinuity or anomaly was detected. On the other hand, a drastic increase of the piezoelectric signal following the rf pulse was noticed in the above temperature range. In the light of recent findings by Gesi,[28] it can be concluded tentatively that a new phase transition with an associated anomaly in the piezoelectric coefficients occurs in $NaNO_2$ at low temperature. More measurements should be performed in order to elucidate the nature of the transition.

The measurements performed at 8 MHz, in order to check on a possible frequency dependence of the relaxation rate, yielded essentially the same results as at 24 MHz in the whole temperature range (see Fig. 3). A small deviation may be present in the paraelectric phase near T_c where the values of $1/T_1$ at 8 MHz seem to be slightly lower. However the experimental error at the lower frequency is considerably greater and consequently a small frequency effect cannot be checked.

Let us focus our attention on the ferroelectric contribution to relaxation which manifests itself by the anomalous increase near T_c. Since the dynamics of the phase transition in $NaNO_2$ must involve a coupling between the lattice and the NO_2^- electric dipole system, the results obtained in Sec. II A for the indirect Raman relaxation process by undamped lattice vibrations will not be applied in this case. On the other hand a relevant direct process should be present and therefore the experimental behavior of $1/T_1$ in the paraelectric region is compared to the theoretical expressions derived in Sec. II B for the ferroelectric contribution associated to a diffusive mode or damped generalized-lattice mode:

$$W \propto (T - T_0)^{-1/2} \quad \text{for isotropic interaction}$$

and

$$W \propto \ln(T - T_0) \quad \text{for anisotropic interaction}.$$

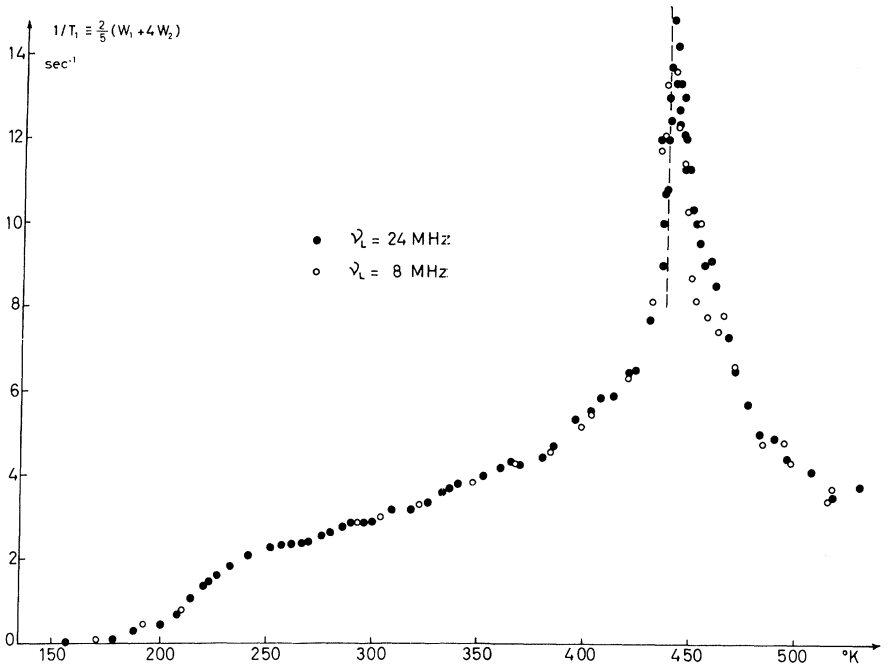

FIG. 3. Relaxation rate $1/T_1 \equiv \frac{2}{5}(W_1+4W_2)$ for Na^{23} in $NaNO_2$ single crystal versus temperature at the resonance frequencies 8 and 24 MHz. The dashed line is drawn to mark the temperature at which the discontinuity in the static dielectric constant occurs.

As is shown in Fig. 4 the experimental data fit a logarithmic expression rather than an inverse power law of the form $(T-T_0)^{-n}$. The best fit of the experimental data yields the following expression for the relaxation rate (for $T_0 = 163\,^\circ$C):

$$\frac{1}{T_1} \equiv \tfrac{2}{5}(W_1+4W_2) = 7.7 \ln\left(\frac{T_0}{T-T_0}\right)^{1/2} - 3.2\ \text{sec}^{-1}. \tag{34}$$

The constants in Eq. (34) contain information about both the microscopic dynamics of the ferroelectric transition and the coupling between the unstable mode and the nuclear-spin system. In order to extract the two types of information separately, measurements of relaxation rate at different resonance frequencies and for different crystal orientations in the external magnetic field were performed. Unfortunately, no appreciable frequency effect was observed and therefore one can infer only that the frequency of the unstable mode is always greater than the Larmor frequency even close to the transition temperature.

While the angular dependence is essentially the same well above and below T_c, it changes appreciably in the neighborhood of the transition. The angular dependence for a rotation of the crystal around the ferroelectric c axis ($\vec{c} \perp \vec{H}_0$) of $W_1 + W_2$ at different temperatures is shown in Fig. 5. Since this was the only angular dependence that could be investigated, the complete form of the efg tensor effective for the relaxation process could not be derived. Nevertheless, some information about the symmetry of the effective efg tensor can be obtained from the available data. Let us define the root mean square of the time fluctuating efg components associated with the

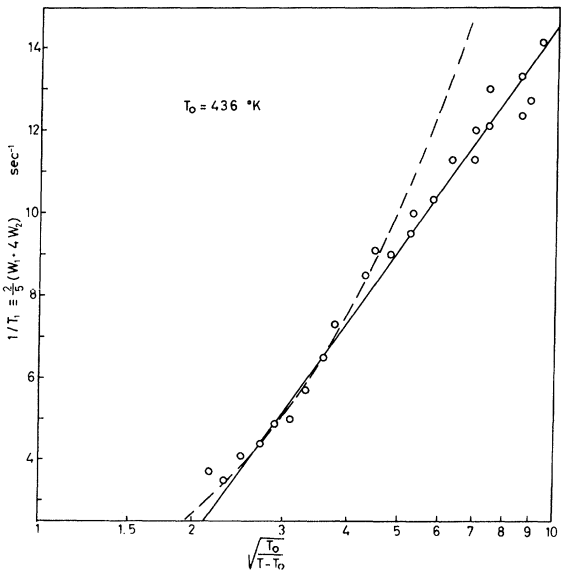

FIG. 4. Semilogarithmic plot of $1/T_1 \equiv \frac{2}{5}(W_1+4W_2)$ versus $[T_0/(T-T_0)]^{1/2}$ for Na^{23} in single crystal $NaNO_2$. The solid straight line represents the function $1/T_1 = 7.7 \times \log [T_0/(T-T_0)]^{1/2} - 3.2$. The dashed line represents the function $1/T_1 = A[T_0/(T-T_0)]^{1/2}$ which is drawn to fit the high-temperature experimental values.

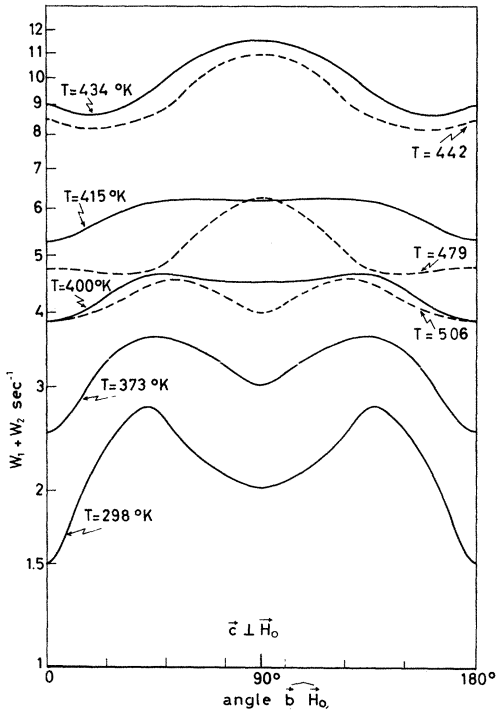

FIG. 5. W_1+W_2 for Na^{23} in single crystal $NaNO_2$ with $\vec{c}\perp\vec{H}_0$ as function of the angle between the b axis and $\vec{H}_0$ at different temperatures; the solid lines refer to $T<T_c$ while the dashed lines refer to $T>T_c$.

ferroelectric unstable mode as the component V_{ij}^F of the efg tensor effective for relaxation.

Since the static efg tensor has the crystal axes as principal axes both above and below T_c,[26] we will tentatively assume that the same is true for the "relaxation-efg tensor" V_{ij}^F. Then for $\vec{c}\perp\vec{H}_0$ and for a rotation about the ferroelectric c axis the relaxation rate W_1+W_2 should have the following angular dependence:

$$W_1+W_2\propto f(\theta,\eta)=(V_{cc}^F)^2\{\eta^2\cos^2\theta\sin^2\theta+\tfrac{1}{4}[\tfrac{1}{2}(3+\eta)-\eta\cos^2\theta]^2\},\quad(35)$$

where θ is the angle between $\vec{H}_0$ and the b axis and $\eta=(V_{aa}^F-V_{bb}^F)/V_{cc}^F$.

The function $f(\theta,\eta)$ is angular independent for $\eta=0$ while for $\eta\neq0$ is a function continuously increasing ($\eta>0$) or decreasing ($\eta<0$) between 0 and $\frac{1}{2}\pi$. The ratio R between the extremal values is

$$R=f(0,\eta)/f(\tfrac{1}{2}\pi,\eta)=[(3-\eta)/(3+\eta)]^2\ .\quad(36)$$

With these assumptions it is found that for $\eta\sim+0.2$ Eq. (35) gives an angular dependence in agreement with the experimental data and a correct ratio between the minimum and maximum value of W_1+W_2, near the phase transition. However it should be pointed out that the minimum displayed by the experimental behavior (see Fig. 5) does not occur exactly at $\theta=0$. This could be due to the presence of a second smaller contribution by a "relaxation-efg tensor" whose principal axes do not coincide with the crystal axes. An additional check of the validity of our conclusions about the symmetry of the "relaxation-efg tensor" is provided by a comparison of the theoretical ratio between W_1+W_2 (for a certain angle θ) and $\frac{2}{5}(W_1+4W_2)$ (for the orientation for which all lines are superimposed) with the corresponding experimental ratio. The relaxation rate for all lines superimposed can be related to the asymmetry parameter and one obtains

$$1/T_1\equiv\tfrac{2}{5}(W_1+4W_2)\propto(V_{cc}^F)^2(0.17\eta^2-0.23\eta+0.68).\quad(37)$$

From Eqs. (37) and (35) one obtains for $\eta=0.2$ a ratio

$$\tfrac{2}{5}(W_1+4W_2)/(W_1+W_2)_{\theta=1/2\pi}\simeq1$$

to be compared with the experimental value of ~1.1 at $T=442$ °K.

At this point one can compare the theoretical expressions (29a) or (29b) with the expression (34) which fits the experimental data. If one considers at first Eq. (29a), which is based on the assumption of a relaxation-type motion, one has, by assuming $\delta=1$, $A=7.7$ sec^{-1} and $\sqrt{\alpha}q_D=1.2$ or 0.85 (according to the two limiting values 0 or 3 sec^{-1} of the "nonferroelectric" background relaxation). The values of α so obtained (2.3 or 1.2 Å^2, respectively) are not in disagreement with the value that can be estimated theoretically using the assumption of an interaction J_{ij} limited to the nearest neighbors. In fact from Eq. (28a) one has $\alpha\simeq\frac{1}{6}\langle d^2\rangle_{av}=2.9$ Å^2 where $\langle d^2\rangle_{av}$ is the mean square value of the nn distance. By using the above experimental values for α one can estimate, from the expression of the constant A [see Eq. (24)], $V_{cc}^F=620$ and 370 KHz, respectively. In the above estimation we have used the value $\tau_0=0.3\times10^{-10}$ sec deduced by Hatta *et al.*[29] from dielectric measurements.

Alternatively let us consider Eq. (29b) which is based on the assumption of a damped generalized soft mode. Assuming $\epsilon\sim\omega_0^2$ and $\gamma\sim\omega_0^2/q_D^2$, and for the quantity $2\Gamma/\omega_0^2$ a value of the order of 10^{-13} sec as can be deduced from reflectivity measurements,[30] one obtains for the efg component V_{cc}^F, a value greater than 10 MHz, which is unreasonable. On the other hand one can obtain a value of $V_{cc}^F\sim500$ KHz if one assumes $2\Gamma/\omega_0^2\equiv\tau_0=0.3\times10^{-10}$ sec, which corresponds to a strongly damped generalized soft mode; in this limit the generalized soft mode is equivalent to a diffusive mode.

Therefore, from the angular and temperature dependence of the relaxation rate it can be concluded that the "relaxation-efg tensor" has its principal axes practically along the crystal axes, with the greatest component $V_{cc}^F \sim 500$ KHz and $\eta = 0.2$. The interpretation of this result in terms of charge and/or electrical dipole localization and of their critical motion is in general very difficult. If one considers the simple picture of NO_2^- dipole cooperative motion, one finds that an efg tensor effective for the relaxation having the principal axes along the crystal axes, with the greatest component V_{cc}^F of the order of the value deduced from the experiment and an asymmetry parameter $\eta \simeq 0.3$, can be obtained by considering the flipping motion along the c axis of three correlated Ising electric dipoles of 0.8×10^{-18} esu localized at the positions $(\pm a, 0, \frac{1}{2}c)$ and $(0, 0, \frac{1}{2}c)$ with respect to the Na^{23} nucleus; (the value of 0.8×10^{-18} esu for the electric dipole component in the c direction is not inconsistent with the values of the atomic dipoles given by Betsuyaku[31] for the NO_2^- group). However no in-phase motion has to occur between two dipoles located at $\vec{r}$ and $-\vec{r}$. In fact, it can be easily seen that two parallel dipoles located at $\vec{r}$ and $-\vec{r}$ do not produce electric field gradients at the origin.

From the above considerations it could be inferred that the critical slowing down involves mainly cooperative modes of the "ferroelectric" dipoles characterized by small wave vectors directed along the a axis.

V. CONCLUDING REMARKS

It has been shown that by studying the quadrupole spin-lattice relaxation in ferroelectric crystals one can detect the presence of unstable generalized lattice modes, since they produce near the transition temperature an anomalous peak in the relaxation rate. The existence of the peak in the relaxation rate can be justified theoretically for the typical microscopic dynamics that are believed to trigger the ferroelectric transition in different type of crystals.

In particular, in $NaNO_2$ the measurements have shown that the rising of the relaxation rate in the transition region (for $T > T_c$) is of logarithmic type. This result points out the importance of taking into account the anisotropic character of the interaction among the "ferroelectric" ions or dipoles.

Measurements as a function of the resonance frequency allow one, in principle, to distinguish between a spectral density characteristic of a relaxation-type motion or of a not-overdamped oscillatory motion, if the critical slowing down reaches the 10^7–10^8-Hz region. In our measurements in $NaNO_2$ no frequency effect was detected. However dielectric dispersion measurements[29] seem to point out that critical motions in the above frequency range are present for temperatures close to T_c. Therefore it would be desirable to perform relaxation measurement very close to T_c with reduced temperature gradients and/or at higher resonance frequency (by using a superconducting magnet).

Note added in proof. It should be noted that also P^{31} dipolar relaxation rate obtained by Blinc and Zumer[8] in KH_2PO_4 can be fitted with a logarithmic-type behavior even close to the transition temperature [see G. Bonera, F. Borsa, and A. Rigomonti, Colloque Ampere, Bucharest, 1970 (unpublished)]. Therefore, the conclusion about the temperature dependence of the damping factor, made by the above authors in the attempt to fit their results, does not seem to be justified. A temperature-independent damping factor is indicated, on the other hand, by Raman spectroscopy results. Furthermore, regarding the new phase transition[28] at 178 °K, measurements of Raman spectra performed by C. K. Asawa and M. K. Barnoski (unpublished report) indicate that no change in crystal symmetry occurs at the transition, in agreement with our observation of no detectable efg changes.

ACKNOWLEDGMENTS

It is a pleasure to acknowledge critical discussions and suggestions by H. Pytte and K. A. Müller, and helpful discussions with R. Blinc and J. L. Bjorkstam. Thanks are also due L. Giulotto for his constant encouragement and interest.

[1]For a review, see, for instance, R. Blinc, *Advances in Magnetic Resonance*, edited by J. S. Waugh (Academic, New York, 1968), Vol. 3, p. 141.

[2]P. W. Anderson, in *Fizika Dielektrikov*, edited by G. I. Skanavi (Akademiia Nauk. SSSR, Moscow, 1960).

[3]W. Cochran, Advan. Phys. 9, 387 (1960).

[4]R. Brout, K. A. Müller, and H. Thomas, Solid State Commun. 4, 507 (1966).

[5]P. G. De Gennes, Solid State Commun. 1, 132 (1963).

[6]K. K. Kobayashi, J. Phys. Soc. Japan 24, 497 (1968).

[7]A. Rigamonti, Phys. Rev. Letters 19, 436 (1967).

[8]R. Blinc and S. Zumer, Phys. Rev. Letters 21, 1004 (1968).

[9]G. Bonera, F. Borsa, and A. Rigamonti, *Proceedings of the Europeon Meeting on Ferroelectricity*, edited by H. E. Müser and J. Peterson (Wissenschaftliche Verlagsgesellschaft MBM, Stuttgart, Germany, 1970), p. 295.

[10]G. Bonera, F. Borsa, and A. Rigamonti, *Magnetic Resonance and Radiofrequency Spectroscopy* (North-Holland, Amsterdam, 1969), pp. 526 and 520; also Phys.

Letters 29A, 88 (1969). Later measurements [G. Bonera, F. Borsa, and A. Rigamonti (unpublished)] of Na^{23} quadrupole relaxation in deuterated Rochelle Salt (kindly supplied by J. L. Bjorkstam) have confirmed the interpretation given in the Phys. Letters work regarding the frequency dependence of the rapid rise of the relaxation rate attributed to the flipping motion of the water molecules.

[11]R. Blinc, S. Zumer and G. Lahajnar, Phys. Rev. B (to be published).

[12]J. Van Kranendonk, Physica 20, 781 (1954).

[13]A. Abragam, *Principles of Nuclear Magnetic* (Oxford U. P., Oxford, 1961).

[14]An evaluation of the second-order contribution in the case of damped phonons is under way by H. Pytte and X. Von der Wardkirch.

[15]See, for example, E. G. Wikner, W. E. Blumberg, and E. L. Hahn, Phys. Rev. 118, 631 (1960); E. G. Weber, *ibid.* 130, 1 (1963); S. K. Joshi, R. Gupta, and T. P. Das, *ibid.* 134, 1693 (1964); F. Bridges and W. G. Clark, *ibid.* 164, 288 (1967).

[16]B. I. Kochelaev, Zh. Eksperim i Teor. Fiz. 37, 242 (1959) [Soviet Phy. JETP 10, 171 (1960)].

[17]Recently, P. Papon and H. Theveneau [Phys. Letters 30A, 362 (1969)] have calculated the relaxation rate near T_c for an anharmonic Raman process. They find a singular behavior as $(T-T_0)^{-3/2}$ by using a dispersion curve of the type $\omega^2=\omega_0^2+aq^2$.

[18]It should be noted that in any case the succeeding terms in the q expansion of $A_\mu(\vec{q})$ do not give singular contributions to the relaxation rate.

[19]M. Suzuki and R. Kubo, J. Phys. Soc. Japan 24, 51 (1968).

[20]K. Tani, J. Phys. Soc. Japan 26, 93 (1969).

[21]E. Pytte and H. Thomas, Phys. Rev. 175, 610 (1968).

[22]The single crystal of sodium nitrite was kindly provided by A. Weiss.

[23]Equations (30) and (31) refer to the case of an axially symmetric efg tensor. For the general case, see M. H. Cohen and F. Reif, in *Solid State Physics*, edited by F. Seitz and D. Turnbull (Academic, New York, 1957), Vol. 5.

[24]For the features of the transition, see S. Tanisaki, J. Phys. Soc. Japan 18, 1181 (1963) and references therein.

[25]It should be pointed out that a para-antiferroelectric transition was reported to occur immediately before the ferroelectric transition [Y. Yamada, I. Shibuya, and S. Hoshino, J. Phys. Soc. Japan 18, 1594 (1963)]. However, the effect of this transition on the dielectric constant is small [K. Gesi, J. Appl. Phys. (Japan) 4, 818 (1965)] and it does not show up in our measurements.

[26]A. Weiss, Z. Naturforsch. 15A, 536 (1960); A. Weiss and D. Biedenkapp, *ibid.* 17A, 794 (1962).

[27]H. Betsuyaku, J. Phys. Soc. Japan 21, 187 (1966).

[28]K. Gesi, J. Phys. Soc. Japan 26, 953 (1969).

[29]I. Hatta, J. Phys. Soc. Japan 24, 1043 (1968); Y. Yamada, Y. Fujii, and I. Hatta, *ibid.* 24, 1053 (1968).

[30]M. K. Barnoski and J. M. Ballantyne, Phys. Rev. 174, 946 (1968).

[31]H. Betsuyaku, J. Chem. Phys. 51, 2546 (1969).

PHYSICAL REVIEW B VOLUME 2, NUMBER 7 1 OCTOBER 1970

Theory of a Two-Dimensional Ising Model with Random Impurities. IV. Generalizations

Barry M. McCoy
Institute for Theoretical Physics, State University of New York, Stony Brook, New York* 11790
(Received 1 June 1970)

In the first paper of this series, we located T_c for an arbitrary distribution of impurity bonds $P(E_2)$ and, for a particular $P(E_2)$ with a narrow width, we found that the specific heat fails to be analytic at T_c, although it is infinitely differentiable there. In this paper, we generalize this conclusion to an arbitrary distribution $P(E_2)$.

I. INTRODUCTION

In the first paper of this series,[1] we introduced a two-dimensional Ising model in which the horizontal energies E_1 are all fixed and all the vertical bonds $E_2(j)$ between the jth row and the $(j+1)$th row are fixed, but $E_2(j)$ is allowed to depend on j. Furthermore, the energies $E_2(j)$ are treated as random variables such that if $j\neq j'$, $E_2(j)$ and $E_2(j')$ are independent and are each described by a temperature-independent probability density $P(E_2)$. For this Ising model, we showed that with probability 1 the thermodynamic limit of the free energy per site exists and is the same for all Ising models of the collection specified by $P(E_2)$.

For this random Ising lattice we located T_c by the general formula

$$0=\int_0^\infty dE_2\,P(E_2)\,\ln\left[z_{2c}^2\left(\frac{1+z_{1c}}{1-z_{1c}}\right)^2\right], \qquad (1.1)$$

where

$$z_i=\tanh\beta E_i\ ,\quad i=1,2 \qquad (1.2)$$

and the subscript c means $T=T_c$. To justify calling the T_c located from (1.1) a critical temperature, we would like to show that the specific heat

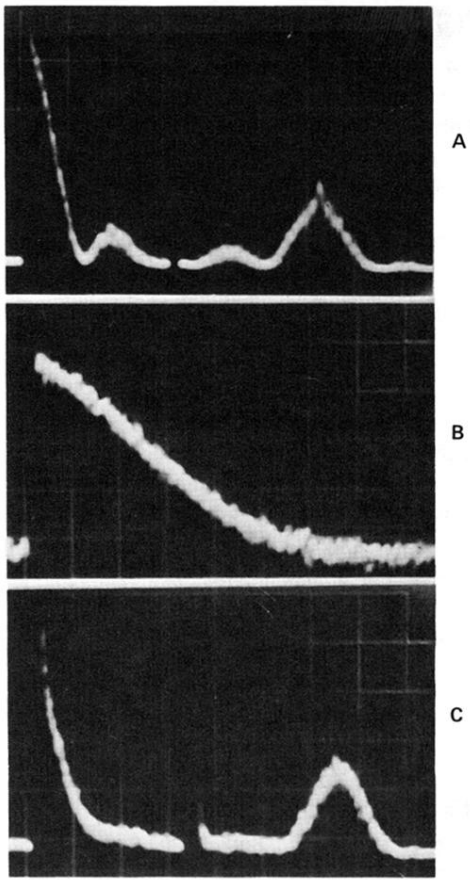

FIG. 1. Na^{23} pulsed NMR signals in $NaNO_2$ at 24 MHz and at room temperature. (a) Free precession (fp) and echo signal in powdered sample with diode detection; (b) fp in single crystal for central-line irradiation; (c) fp and echo in single crystal for a satellite-line irradiation. (The time base is 100 μs/div.)